Physical Science International Journal

Volume 26, Issue 8, Page 46-54, 2022; Article no.PSIJ.95554
ISSN: 2348-0130

Three-dimensional Modeling Study of the Effect of Irradiation on a Single-face Polycrystalline Silicon Photocell under Multispectral Illumination

Mayoro Dieye [a*], Nacire Mbengue [a,b] and Awa Dieye [a,b]

[a] Department of Physic, Science Faculty, Semiconductor Optoelectronics Group (GOES), University Cheikh anta Diop of Dakar (UCAD), BP-5005, Senegal.
[b] Department of Physic, Science Faculty, Solar Energy Materials and Systems Laboratory (LASES), University Cheikh anta Diop of Dakar (UCAD), BP-5005, Senegal.

Authors' contributions

This work was carried out in collaboration among all authors. All authors read and approved the final manuscript.

Article Information

DOI: 10.9734/PSIJ/2022/v26i8760

Open Peer Review History:
This journal follows the Advanced Open Peer Review policy. Identity of the Reviewers, Editor(s) and additional Reviewers, peer review comments, different versions of the manuscript, comments of the editors, etc are available here: https://www.sdiarticle5.com/review-history/95554

Original Research Article

Received: 27/10/2022
Accepted: 30/12/2022
Published: 31/12/2022

ABSTRACT

A three-dimensional modeling study of a polycrystalline silicon mono-facet photocell under multi-spectral illumination is presented highlighting the effect of irradiation energy (Φ) and damage coefficient (Kl) on the macroscopic parameters. Using the junction recombination rate Sf and the backside recombination rate (Sb) in a 3D modeling study, the continuity equation is solved. We determined the current density the current density and the photovoltage. This study takes into account the irradiation energy and the damage coefficient on the quality of the polycrystalline silicon photocell.

**Corresponding author: E-mail: Yoroma90@gmail.com;*

Keywords: Grain size; grain boundary recombination velocity; polycrystalline; solar cell; irradiation; current density; photovoltage.

1. INTRODUCTION

To increase the efficiency of solar cells, a number of techniques for characterising the silicon material and determining the phenomenological and electrical characteristics have been employed.

Some of these methods were created in the static regime [1] while others were created in the dynamic frequency regime [2]. Extensive studies on the capacity of the space charge area [3,4] and recombination parameters [5,6] have been performed in 3 dimensions [1,6,7,8-10] for these two regimes. Our contribution consists in determining the current density and photovoltage of a silicon photocell in static regime placed under (Kl, Φ) irradiation and multi-spectral illumination.

We briefly outline a theoretical investigation in which we model a photocell grain and solve the diffusion equation. We then talk about the outcomes before coming to a conclusion.

2. THEORITICAL ANALYSIS

The bifacial solar cell is a device that generates electricity directly from visible light. When light quanta are absorbed, electron-hole pairs are generated as can be seen in Fig. 1.a. A studied BSF polycrystalline silicon solar cell is an n+-p-p+ structure, composed of many small individual grains, is considered as shown in Fig. 1.b below [6,11,12].

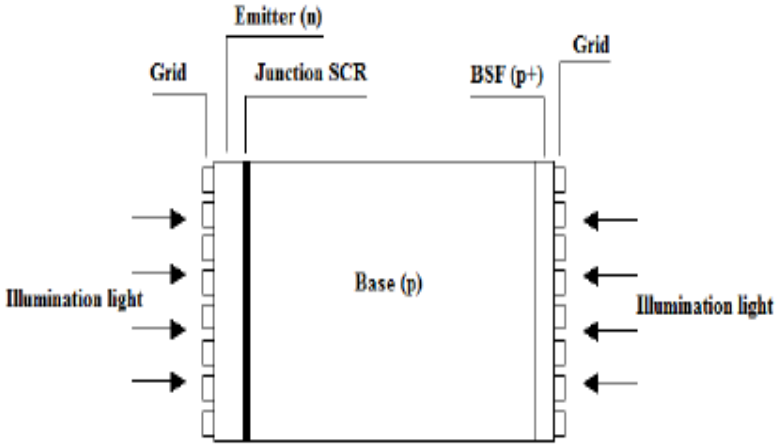

Fig. 1a. Bifacial Silicon solar cell Structure

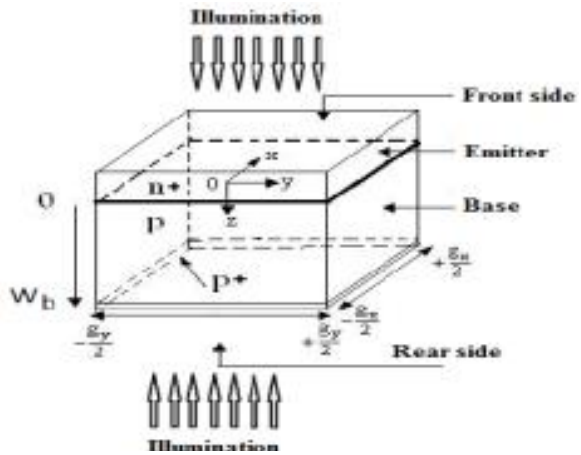

Fig. 1b. Polycristalline Silicon columnar grain model

In this study, we assume that:

- The contribution of the emitter is neglected. We take into account only the base contribution [6],
- The generation rate of electron-hole pairs depends only on the base depth z [12];
- The existing crystalline field within the base is neglected
- In the simulation, we have equality between the grain size along x and y axes, ie gx= gy=g(square cross section), and that the recombination velocity at grain boundaries is perpendicular to the junction and independent to the generation rate under AM 1.5 [6-9].

2.1 Excess Minority Carriers Density

The emitter of the solar cell is considered as a dead zone (not active). Thus the minority charge carrier density is derived from the continuity equation considering only the contribution of the base of the solar cell [6-14]:

$$D(Kl,\phi)\times\left[\frac{\partial^2\delta(x,y,z)}{\partial x^2}+\frac{\partial^2\delta(x,y,z)}{\partial y^2}+\frac{\partial^2\delta(x,y,z)}{\partial z^2}\right]-\frac{\delta(x,y,z)}{\tau}+G(z)=0 \quad (1)$$

$D(Kl,\phi)$ is the diffusion coefficient in the presence of irradiation. It is expressed as follows:

$$D(Kl,\phi)=\frac{L(Kl,\phi)^2}{\tau} \quad (2)$$

In this expression, G(z) represents the generation rate of minority charge carriers in the base [15] whose expression is given by the following equation:

$$G(z)=\sum_{i=1}^{3} a_i\times\exp\left(-b_i\times z\right) \quad (3)$$

The values ai and bi are the values tabulated from the modeling of the absorption spectrum of the photocell for AM 1.5 [9,11,19].

L depend on the irradiation energy Φ and the damage coefficient Kl through the following expression [19]-[21]:

$$L(Kl,\phi)=\sqrt{\frac{1}{\frac{1}{L_0^2}+Kl\times\phi}} \quad (4)$$

L_0 is the diffusion length without irradiation.

The solution of the equation can be written as follows [6,9,22]:

$$\delta(x,y,z)=\sum_k\sum_j Z_{k,j}(z)\times\cos(C_k\times x).\cos(C_j\times y) \quad (5)$$

k, j : are the indices for the x and y directions respectively.

Ck and Cj are obtained from the conditions at the grain boundaries $\pm\frac{g_x}{2}$ et $\pm\frac{g_y}{2}$ [6-9-11-23]:

$$\left[\frac{\partial\delta(x,y,z)}{\partial x}\right]_{x=\pm\frac{g_x}{2}}=\mp\frac{Sgb}{D(Kl,\phi)}\delta\left(\pm\frac{g_x}{2},y,z\right) \quad (6)$$

$$\left[\frac{\partial\delta(x,y,z)}{\partial y}\right]_{y=\pm\frac{g_y}{2}}=\mp\frac{Sgb}{D(Kl,\phi)}\delta\left(x\pm\frac{g_y}{2},z\right) \quad (7)$$

gx is the grain width, gy the grain length Sgb the recombination velocity at the grain boundaries. From equations (6) and (7) we obtain two transcendental equations [30] which are:

$$\tan\left(C_k\times\frac{g_x}{2}\right)=\frac{Sgb}{2.C_k\times D(Kl,\phi)} \quad (8)$$

$$\tan\left(C_j\times\frac{g_y}{2}\right)=\frac{Sgb}{2.C_j\times D(Kl,\phi)} \quad (9)$$

By replacing δ(x, y, z) in the continuity equation and the fact that the cosine function is orthogonal, we obtain the following differential equation:

$$Z_{k,j} = A_{k,j} \times \cosh\left(\frac{z}{L_{k,j}}\right) + B_{k,j} \times \sinh\left(\frac{z}{L_{k,j}}\right) - \sum_{i=1}^{3} K_{i,j,k} \times \exp\left(-b_i \times z\right) \quad (10)$$

Or

$$K_{i,j,k} = \frac{L_{k,j}^2}{D_{k,j} \times \left[b_i^2 \times L_{k,j}^2 - 1\right]} \times a_i \quad (11)$$

With :

$$L_{k,j} = \left[C_k^2 + C_j^2 + \frac{1}{L(Kl,\phi)^2}\right]^{-\frac{1}{2}} \quad (12)$$

And

$$D_{k,j} = D(Kl,\phi) \times \frac{\left[C_k \times g_x + \sin\left(C_k \times g_x\right)\right]\left[C_j \times g_y + \sin\left(C_j \times g_y\right)\right]}{16 \cdot \sin\left(C_k \times \frac{g_x}{2}\right) \cdot \sin\left(C_j \times \frac{g_y}{2}\right)} \quad (13)$$

The coefficients Ak,j and Bk,j are calculated from the following boundary conditions [2-6-10-15-27]:

- At the junction ($z = 0$) :

$$\left[\frac{\partial \delta(x,y,z)}{\partial z}\right]_{z=0} = \frac{Sf}{D(Kl,\phi)} \delta(x,y,0) \quad (14)$$

For each illumination mode, the intrinsic junction recombination velocity was calculated using the method described in

At the back side ($z = \omega b$):

$$\left[\frac{\partial \delta(x,y,z)}{\partial z}\right]_{z=0} = -\frac{Sb}{D(Kl,\phi)} \delta(x,y,\omega b) \quad (15)$$

Sb is the back surface recombination velocity. It quantifies the rate at which excess minority carriers are lost at the back surface of the cell [2-6-10-27]. The derivation of the photocurrent with respect to Sf, provides for each illumination mode the expression of Sb,

$$A_{k,j} = \sum_{i=1}^{3} K_{i,k,j} \times \frac{\frac{1}{L_{k,j}} + \left(\frac{Sf}{D(Kl,\phi)} - b_i\right) \times \exp\left(-b_i \times \omega b\right) + Y_{k,j}\left(\frac{Sf}{D(Kl,\phi)} + b_i\right)}{\frac{Sf \times Y_{k,j}}{D(Kl,\phi)} + \frac{X_{k,j}}{L_{k,j}}} \quad (16)$$

$$B_{k,j} = \sum_{i=1}^{3} K_{i,k,j} \times \frac{\frac{Sf}{D(Kl,\phi)} + \left(\frac{Sb}{D(Kl,\phi)} - b_i\right) \times \exp\left(-b_i \times \omega b\right) + X_{k,j}\left(\frac{Sf}{D(Kl,\phi)} + b_i\right)}{\frac{Sf \times Y_{k,j}}{D(Kl,\phi)} + \frac{X_{k,j}}{L_{k,j}}} \quad (17)$$

With:

$$B_{k,j} = \sum_{i=1}^{3} K_{i,k,j} \times \frac{\frac{Sf}{D(Kl,\phi)} + \left(\frac{Sb}{D(Kl,\phi)} - b_i\right) \times \exp\left(-b_i \times \omega b\right) + X_{k,j}\left(\frac{Sf}{D(Kl,\phi)} + b_i\right)}{\frac{Sf \times Y_{k,j}}{D(Kl,\phi)} + \frac{X_{k,j}}{L_{k,j}}}$$

$$X_{k,j} = \frac{1}{L_{k,j}} \times \sinh\left(\frac{\omega b}{L_{k,j}}\right) + \frac{Sb}{D(Kl,\phi)} \times \cosh\left(\frac{\omega b}{L_{k,j}}\right) \quad (18)$$

$$Y_{k,j} = \frac{1}{L_{k,j}} \times \cosh\left(\frac{\omega b}{L_{k,j}}\right) + \frac{Sb}{D(Kl,\phi)} \times \sinh\left(\frac{\omega b}{L_{k,j}}\right) \quad (19)$$

2.2 Photocurrent Density

The photocurrent density can be calculated by the following equation [6-9-12-28-29].

$$J_{ph} = \frac{q \times D(Kl,\phi)}{g_x \times g_y} \cdot \int_{-\frac{g_x}{2}}^{+\frac{g_x}{2}} \int_{-\frac{g_y}{2}}^{+\frac{g_y}{2}} \left[\frac{\partial \delta(x,y,z)}{\partial z}\right]_{z=0} dx.dy \quad (20)$$

After calculation we get:

$$J_{ph}(Sf,Kl,\phi) = q \times \sum_{k=1}^{5}\sum_{j=1}^{5} R_{k,j} \times Sf \cdot \sum_{i=1}^{3} K_{i,k,j} \cdot \frac{\frac{Sb - D(Kl,\phi) \times b_i}{D(Kl,\phi) \times Y_{k,j}} - \frac{X_{k,j}}{Y_{k,j}} + b_j \times L_{k,j}}{\frac{X_{k,j}}{Y_{k,j}} + \frac{Sf \times L_{k,j}}{D(Kl,\phi)}} \quad (21)$$

With, $$R_{k,j} = \frac{4 \cdot \sin\left(C_k \times \frac{g_x}{2}\right) \times \sin\left(C_k \times \frac{g_y}{2}\right)}{g_x \times g_y \times C_k \times C_j} \quad (22)$$

q is the charge of the electron.

2.3 Photo Voltage

Using the Boltzmann's relation, the photo voltage Vph can be expressed as [6,9,28]:

$$V_{ph} = V_T \cdot \ln\left\{1 + \frac{N_b}{n_i^2} \cdot \int_{-\frac{g_x}{2}}^{+\frac{g_x}{2}} \int_{-\frac{g_y}{2}}^{+\frac{g_y}{2}} \delta(x,y,z).dx.dy\right\} \quad (23)$$

When the photocell is illuminated simultaneously by the front and rear sides, the photovoltage is given by the following expression:

$$V_{ph} = V_T \cdot \ln\left\{1 + \frac{N_b}{n_i^2}\sum_{k=0}^{4}\sum_{j=0}^{4} R_{k,j}\cdot\sum_{i=1}^{3} K_{i,k,j}\cdot\frac{\frac{Sb - D(Kl,\phi)b_j}{D(Kl,\phi)Y_{k,j}}\cdot\exp\left(-b_j\times H\right) - \frac{X_{k,j}}{Y_{k,j}} + b_j\times L_{k,j}}{\frac{X_{k,j}}{Y_{k,j}} + \frac{Sf\times L_{k,j}}{D(Kl,\phi)}}\right\} \quad (24)$$

$V_T = \frac{k \times T}{q}$ is the thermal voltage, k the Boltzmann constant, Nb the base doping rate and ni the intrinsic carrier concentration.

3. RESULTS AND DISCUSSIONS

3.1 Effect of the Irradiation Energy on the Current Density

The Fig. 2 plots the current density as a function of the recombination velocity at the junction, of a front-illuminated photocell. We considered increasing irradiation energies Φ, grain sizes, recombination velocities at the grain boundaries and damage coefficients are fixed.

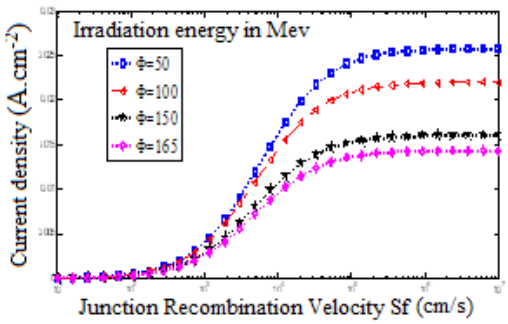

Fig. 2. Current density as a function of the recombination rate at the Sfj junction for a grain size g=0.0005 cm and different irradiation energies, Sgb=4,5*10^{6}cm/s; Kl=10,5 cm^{-2}/MeV; ωb=0.03 cm and AM 1.5

The current density increases with the recombination rate at the junction. The evolution of the current density presents two remarkable levels:

- One in an open-circuit situation where the current density is almost zero,
- The other in short-circuit situation where the current density is maximum.

Between the two situations mentioned above, the operating point of the solar cell varies. The increase of the irradiation energy leads to a decrease of the amplitude of the current density. The explanation that can be drawn from this is that the irradiation energy reduces the mobility of the carriers at the junction. But also, it blocks the carriers, thus, the concentration of the carriers increases, hence a decrease of the current density.

3.2 Effect of the Damage Coefficient Kl on the Current Density

We plot in the following Fig. 3 the current density versus the recombination rate at the junction for different damage coefficients. For this, we fix the grain size, the recombination velocity at the grain boundary and the irradiation energy.

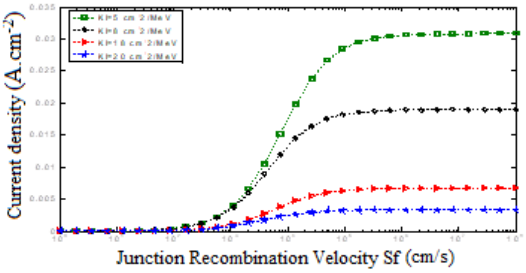

Fig. 3. Current density as a function of recombination rate at the Sfj junction for grain size g=0.0005 cm and different damage coefficients, Sgb=4,5*10^{6}cm/s; Φ=150 MeV; ωb=0.03 cm and AM 1.5

In Fig. 2 we show the curves of the current density versus the recombination rate at the junction as the damage coefficient varies.

We noted that the current density decreases when the damage coefficient increases. This increase is more important for the values of the damage coefficient higher than 8 cm^{-2} /MeV.

The evolution towards this situation characterizes that the increase of the damage coefficient reflects an increase in the probability of creation of defects by irradiation, thus of more important degradation of the solar cell, i.e., more important leakages.

3.3 Effect of the Irradiation Energy on the Photovoltage

The Fig. 4 represents the photovoltage as a function of the recombination rate at the junction of the same solar cell illuminated by four increasing irradiation energies.

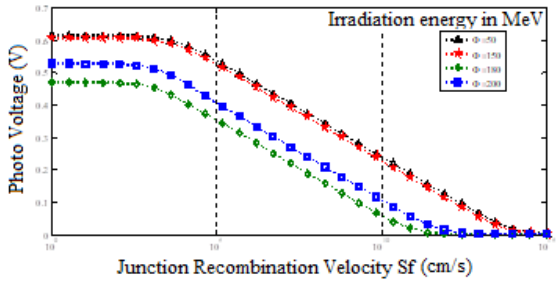

Fig. 4. Photovoltage versus recombination rate at the Sfj junction for a grain size g= 0.0005cm and different irradiation energies, Sgb=4,5*10^{6}cm/s; Kl=10,5 cm^{-2}/MeV ; ωb=0.03 cm and AM 1.5

The curves Fig. 4 of photovoltage versus Sfj for different values of the irradiation energy show levels for low recombination rates at the junction, in this area the photovoltage is maximum. It corresponds to the open circuit. There is storage of carriers at the junction. However, when the speed of recombination exceeds a certain value, the photovoltage which coincides with the limit of the zero current density, decreases very quickly to cancel at high speeds of recombination at the junction Sfj: this is the operation of the photocell in short-circuit which is a point of operation where the photocell delivers a maximum current and a zero voltage

From this figure, we note that the phototension decreases when the irradiation energy increases.

The passage of a charged particle, particularly an ion, through the material causes damaged regions along its path, which become centres of carrier trapping. Irradiation causes intrinsic defects due to the interaction of charged particles with silicon electrons. The charged particles lose energy in the material, resulting in a decrease in photovoltage. Indeed, if the irradiation energy increases, it means that the material becomes more sensitive to degradation caused by possible particles and therefore the photo tension will be more degraded as the irradiation energy increases.

3.4 Effect of the Irradiation Energy on the Photovoltage

We plot in the following Fig. 5 the photovoltage versus the recombination rate at the junction for different damage coefficients. For this purpose, we fix the grain sizes, the recombination rate at the grain boundaries and the irradiation energy.

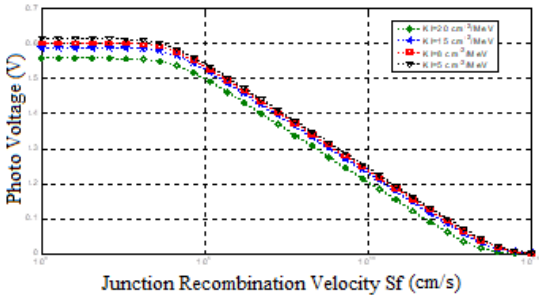

Fig. 5. Photovoltage as a function of recombination rate at the Sfj junction for grain size g= 0.0005 cm and different damage coefficients, Sgb=4.5*10^{6}cm/s; Φ=150 MeV, ωb=0.03 cm and AM 1.5

Let us note on Fig. 5 that this decrease of the photovoltage is especially marked when the photocell works in the vicinity of the open circuit; indeed, in the vicinity of the open the carriers are stored near the junction, which increases the probability of interaction with the irradiating particles and thus the degradation.

3.5 Effect of the Irradiation Energy Φ on the I-V Characteristic of the Photocell

The current-voltage characteristic giving the profile of the current density as a function of photovoltage when Sfj varies and for different values of the irradiation energy when the grain size, the recombination rate at the grain boundaries and the damage coefficient are fixed.

Fig. 6 represents the evolution of the current density as a function of photovoltage by varying the irradiation energy.

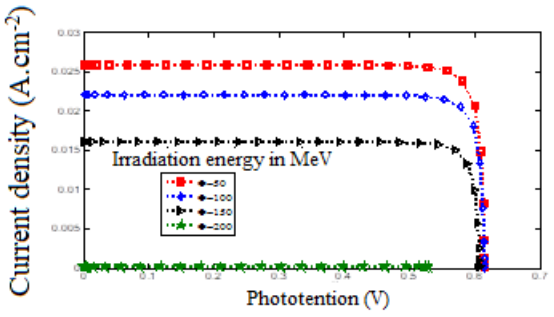

Fig. 6. Current density as a function of photo voltage for grain size g=0.0005 cm and different irradiation energies, Sgb=4,5*10^{6}cm/s; Kl=10,5 cm^{-2}/MeV ; ωb=0.03 cm and AM 1.5

We observe here that the current-voltage characteristic decreases with the irradiation energy; indeed, when the irradiation energy increases, the degradations caused are more important within the material which leads to a decrease of the current density and the photovoltage.

3.6 Effect of the Damage Coefficient Kl on the I-V Characteristic of the Photocell

We plot in Fig. 7 the current-voltage characteristic of the bifacial photocell illuminated by its front side for different values of damage coefficients.

This Fig. 7 shows the effect of the damage coefficient on the open circuit and the short circuit.

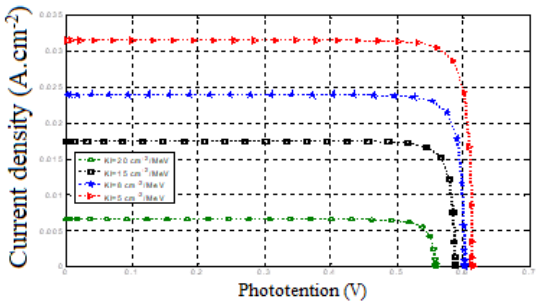

Fig. 7. Current density as a function of photo voltage for grain size g=0.0005 cm and different damage coefficient values, Sgb=4,5*10^{6}cm/s; Φ=150 MeV ; ωb=0.03 cm and AM 1.5

We can always note on the Fig. 7 that the current-voltage characteristic decreases with the damage coefficient; this decrease being more accentuated for the high damage coefficients. Indeed, if the damage coefficient increases, it means that the material becomes more sensitive to degradation caused by particles and therefore the current density and photovoltage will be more degraded as the damage coefficient increases.

4. CONCLUSION

The density of minority charge carriers, the current density and the photoelectric voltage of the photoelectric cell, it is estimated.

Using the Sf junction recombination velocity concept allows us to determine the current density and photovoltage of the solar cell for any operating point of the solar cell.

The effect of irradiation (Φ and Kl) is different for low Sf values (0-10 3) m/s and high Sf m/s, which characterizes the two operating modes.

It is shown that, for any real operating point, the current density and photovoltage of the solar cell decrease with irradiation (Φ and Kl).

It appears that the degradations caused depend of course on the coefficient of damage which amplifies them and on the irradiation energy; for the irradiation energy, it seems that its effect is especially marked beyond a threshold of about 10 MeV. From this threshold, the effects are exacerbated.

COMPETING INTERESTS

Authors have declared that no competing interests exist.

REFERENCES

1. Samb ML, Sarr S, Mbodji S, Gueye S, Dieng M, Sissoko G. Study in 3-D modeling of a silicon photocell in static regime under multispectral illumination multispectral: determination of the electrical parameters. J Sci. 2009;9(4):36-50.
   Available: http ://www.cadjds.org
2. Mbodji S, Maiga AS, Dieng M, Wereme A, Sissoko G. Renoval charge technic applied to a bifacial solar cell under constant magnetic field. Glob J Pure Appl Sci. 2010;15(N0. 4):469-77.
3. Madougou S, Nzonzolo S, Mbodji F. Barro and G. Sissoko. J Sci. 2004 , Bifacial silicon solar cell space charge region width determination by a study in modelling: effect of the magnetic field;4(3):116-23.
4. Barro FI, Mbodji S, Ndiaye M, Ba E, Sissoko G. Influence of grains size and grains boundaries recombination on the space-charge layer thickness z of emitter-base junction's n+-p-p+ solar cell. p. 604-7; 2008-1CV.2.63.
   Available: http://www.eupvsec. Proceedings of the 23rd European photovoltaic solar energy conference. Available from: proceedings.com. doi: 10.4229/23rdEUPVSEC
5. Samb ML, Dieng M, Mbodji S, Mbow B, Thiam N, Barro FI et al.

Recombinationparameters measurement of silicon solar cell under constant white bias light. Proceedings of the 24th European photovoltaic solar energy conference. 2009;469-72.
Available:http://www.eupvsec-proceedings.com.
DOI: 10.4229/24thEUPVSEC2009-1CV.4.15

6. Diallo HL, Seïdou Maiga A, Wereme A, Sissoko G. New approach of both junction and back surface recombination velocities in a 3D modeling study of a polycrystalline silicon solar cell. Eur Phys J Appl Phys. 2008;42(3):203-11.
DOI: 10.1051/epjap:2008085
7. Dieng ML, Sow S, Mbodji ML, Samb M, Ndiaye M, Thiame FI. Barro and G. Sissoko. 3D Study of a Polycrystalline Silicon Solar Cell: influence of Applied Magnetic Field on the Electrical Parameters. Proceedings of the 24th EuropeanPhotovoltaic solar energy conference. 2009;473-6.
Available: http://www.eupvsec-proceedings.com.
DOI: 10.4229/24thEUPVSEC2009-1CV.4.16
8. Zouma B, Maiga AS, Dieng M, Zougmore F, Sissoko G. 3D Approach of spectral response for a bifacial silicon solar cell under a constant magnetic field. Glob J Pure Appl Sci. 2009;15(1):117-24.
DOI: 10.4314/gjpas.v15i1.44908
9. Dugas J. 3 D Modelling of a Reverse Cell Made with improved Multycrystalline Silicon Wafers. Sol Energy Mater Sol Cells. 1994;32(1):71-88.
DOI: 10.1016/0927-0248(94)90257-7
10. Mbodji S, Dieng M, Mbow B, Barro FI, Sissoko G. Three dimensional simulated modelling of diffusion capacitance of polycrystalline bifacial silicon solar cell. Appl Sci Technol (JAST). 2010;15(1-2):109-14.
DOI: 10.4314/jast.v15i1-2.54834
11. Dhariwal SR, Mehrotra DR. Photocurrent and photovoltage from polycrystalline p-n junction Solar Cells. Solar Cells. 1988;25(3):223-33.
DOI: 10.1016/0379-6787(88)90062-2
12. El Ghitani H, Martinuzzi S. Influence of dislocations on electrical properties of large grained polycrystalline silicon cells. I. Model. J Appl Phys. 1989;66(4):1717-22.
DOI: 10.1063/1.344392
13. Saritas M, Mckell HD. Comparison of minority-carrier diffusion length measurements in silicon by the photoconductive decay and surface photovoltage methods. J Appl Phys. 1988;63(9):4561-7.
DOI: 10.1063/1.340155
14. Mbodji S, Mbow B, Barro FI, Sissoko G. A 3D model for thickness and diffusion capacitance of emitter-base junction determination in a bifacial polycrystalline solar cell under real operating condition. Turk J Phys. 2011;15:281-91.
DOI: 10.3906/fiz-0911-25
15. Furlan J, Amon S. Approximation of the carrier generation rate in illuminated silicon. Solid State Electron. 1985;28(12):1241-3.
DOI: 10.1016/0038-1101(85)90048-6
16. Walters RJ, Summers GP. Space radiation effects in advanced solar cell materials and devices mat. Proceedings of the Vol. Res Soc Symp. 2002;692:569-80.
17. Ould El Moujtaba MA, Ndiaye M, Diao A, Thiame M, Barro IF, Sissoko G. Theoretical study of the influence of irradiation on a silicon solar cell under multispectral illumination. Res J Appl Sci Eng Technol. 2002;4(23):5068-73.
18. Ahrenkiel RK, Dunlavy DJ, Hamaker HC, Green RT, Lewis CR, Hayes RE et al. Time-of-flight studies of minority-carrier diffusion in AlxGa1-xAs homojunctions. Appl Phys Lett. 1986;49(12):725-7.
DOI: 10.1063/1.97580
19. Oualid J, Singal CM. Influence of illumination on the grain boundaries recombination velocity in silicon. J Appl Phys. 1984;55(4):1195-205.
20. Dieng A, Thiam N, Samb ML, Maïga AS, Barro FI, Sissoko G. 3rd study of a polycrystalline silicon photocell influence of grain size and recombination rate at the grain boundaries on the electrical grain boundaries on the electrical parameters. J Sci. 2009;9(N0) 1:51-63. org.
21. Shimizu H, Kinamery K, Honma N, Japanese CM. Determination of Surface Charge and Interface Trap Densities in Naturally Oxidize n-type Si Wafers Using Surface Photovoltages. J Appl Phys. 1987;26:2033-6.
22. Halder NC, Williams TR. Grain boundary effects in polycrystalline Silicon SolarCells I. Solution of the three- Dimensional diffusion equation by the Green's function method. Sol Cells. 1983;8(3):201-23.

DOI: 10.1016/0379-6787(83)90061-3
23. Nzonzolo L-B, D, Mabika CN, Sissoko G. Two- dimensional finite element method analysis effect of the recombination velocity at the grain boundaries on the characteristics of a polycrystalline silicon solar cell. Circuits Syst. 2016;7:4186-200. DOI: 10.4236/cs.2016.713344
24. Sissoko G, Nanéma E, Corréa A, Biteye PM, Adj M, Ndiaye AL. Silicon Solar cell recombination parameters determination using the characteristic. Renew Energy, 0960-1481/98/#. 1998;3:1848-185.1.
25. Sissoko G, Museruka C, Correa A, Gaye I, Ndiaye AL. Light spectral effect on recombination parameters of silicon solar cell. In: Proceedings of the world renewable energy congress, Denver, USA. 1996:1487-90.
26. Bocande YLB, Correa A, Gaye I, Sow ML, Sissoko G. Bulk and surfaces parameters determination in high efficiency Si solar cells. Renew Energy, 0960-1481. 1994;5(III):1698-700.
27. Ndiaye M, Diao A, Thiame M, Dione MM, LY H, Diallo ML et al. 3D approach for a modelling study of the diffusion capacitance's efficiency of the solar cell. In: Proceedings of the 25th European photovoltaic solar energy conference and exhibition, Valencia, Spain. 2010;484-7.
28. Dione MM, Ly I, Diao A, Gueye S, Gueye A, Thiame M et al. Determination of the impact of the grain size and the recombination velocity at grain boundary on the values of the electrical parameters of a bifacial polycristallin silicon solar cell, IRACST – engineering Science and Technology [international journal]. 2013;3(N0. 1):66-73.
29. Ben Arab A. Photovoltaic properties and high efficiency of preferentially doped polysilicon solar cells. Solid State Electron. 1995;38(8):1441-7. DOI: 10.1016/0038-1101(94)00283-L
30. Deme MM, Mbodji S, Ndoye S, Thiam A, Dieng A, GS. Influence of illumination incidence angle, grain size and grain boundary recombination Velocity on the facial solar cell diffusion capacitance; Revue des Energies Renouvelables.. 2010;13(1):109-21.

Peer-review history:
The peer review history for this paper can be accessed here:
https://www.sdiarticle5.com/review-history/95554